

Polarization Patterning and Single-Point PFM Spectroscopy

A. Gruverman

University of Nebraska-Lincoln, USA

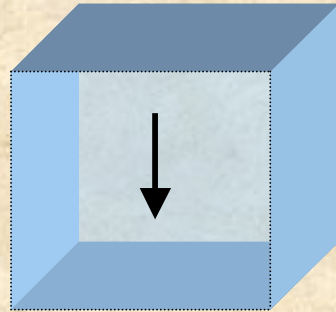
**EPFL Workshop on Piezoresponse Force Microscopy
Lausanne, Switzerland
May 26-28, 2008**

Outline

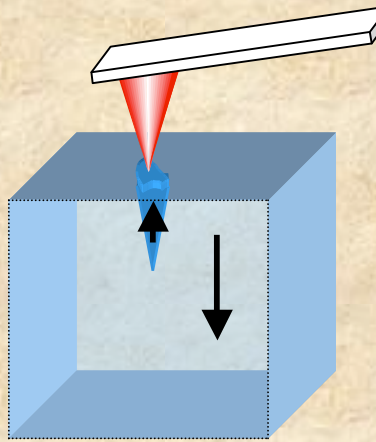
- ◆ **Introduction**
- ◆ **Single-point Spectroscopy in PFM**
*Bias dependent measurements: local vs global excitation
Local spectroscopy of capacitors and nanostructures*
- ◆ **Ferroelectric Switching in Tip-Induced Field**
Effect of crystallographic orientation and defects on local hysteresis
- ◆ **PFM for Domain Growth Studies**
Time-dependent measurements in non-uniform electric field
- ◆ **“Anomalous” Polarization Switching in PFM**
Effect of poling conditions and material properties
- ◆ **Domain Patterning and Ferroelectric Templates**
Nucleation vs wall motion
- ◆ **Conclusion**

Mechanism of Switching in PFM

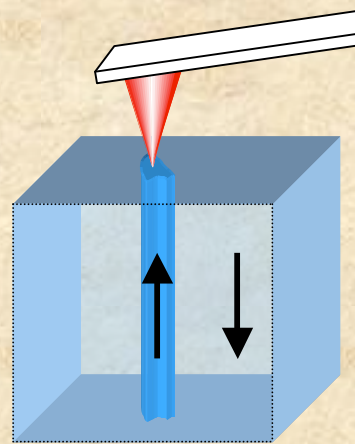
**Local switching
(tip-induced)**



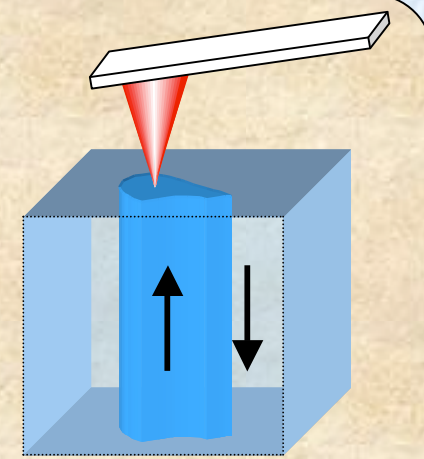
initial state



nucleation

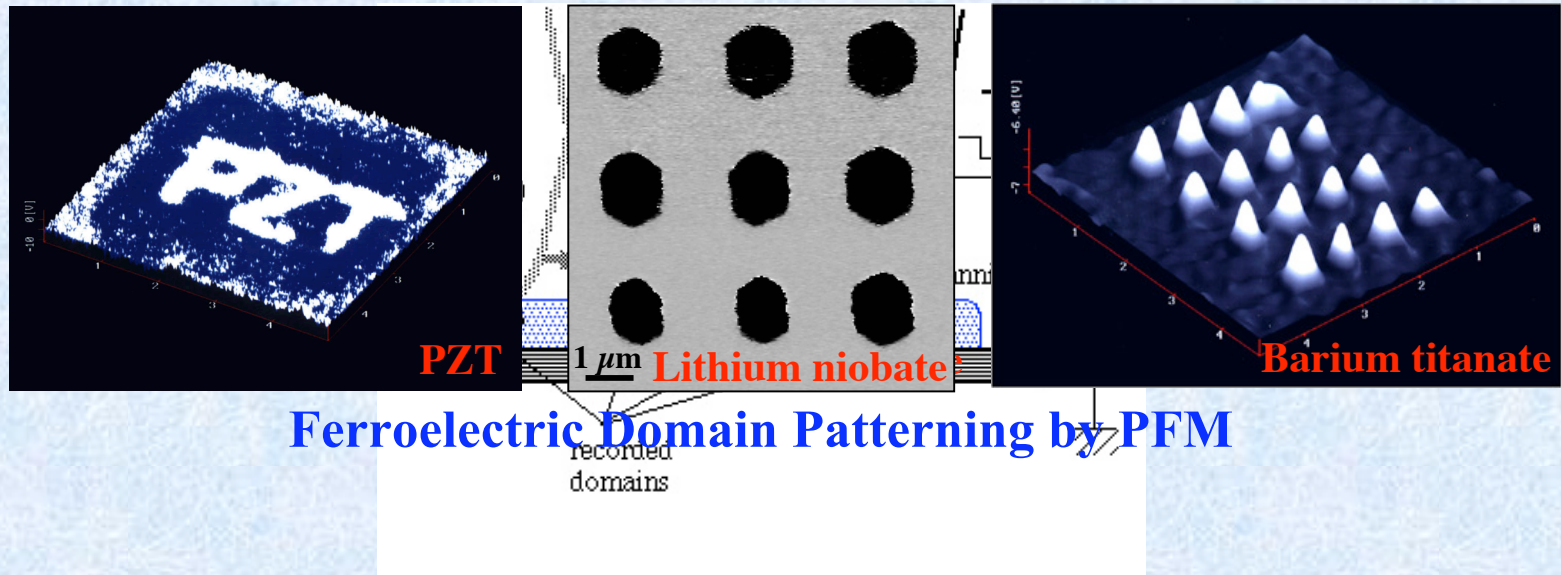


forward growth

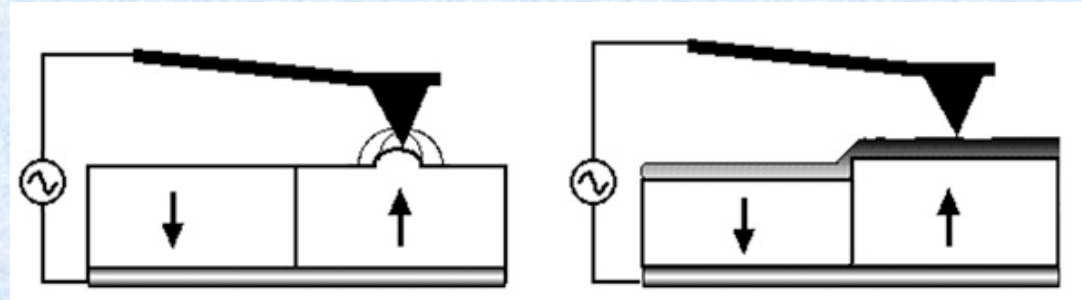


lateral expansion

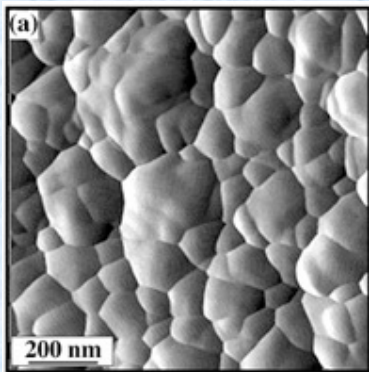
Nanoscale Domain Patterning



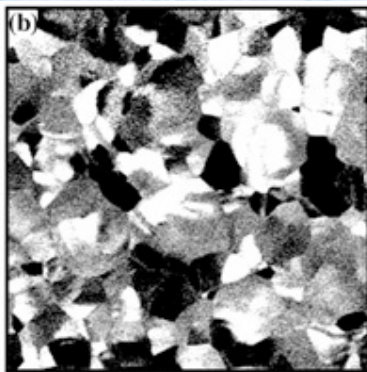
PFM Imaging: Local vs Integral Excitation



PZT thin film

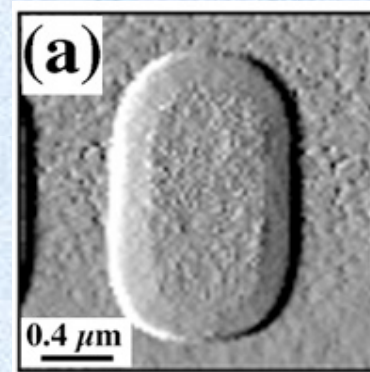


Topography

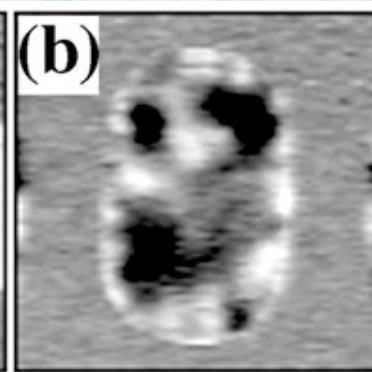


Piezoresponse

PZT capacitor



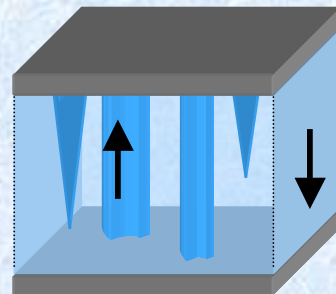
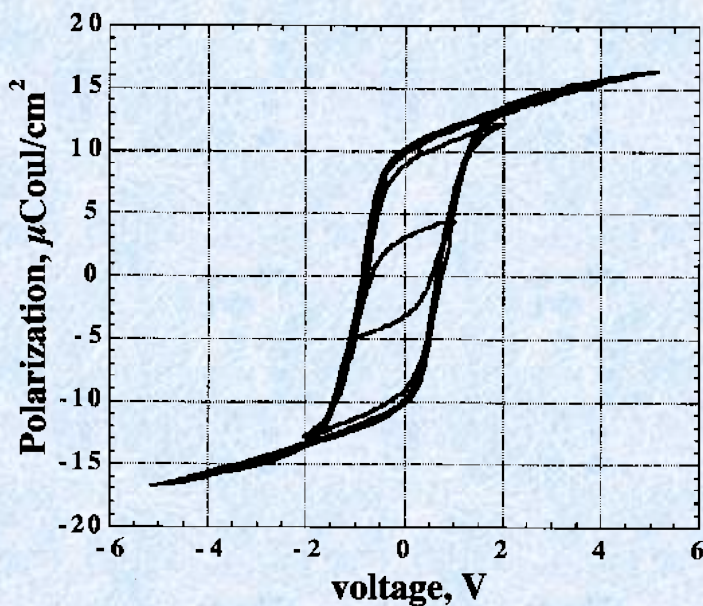
Topography



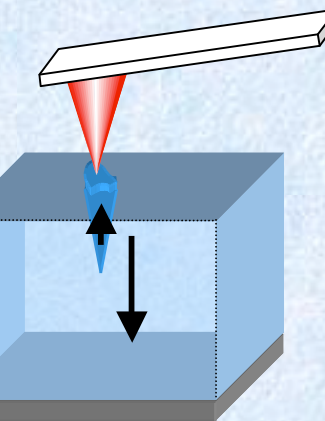
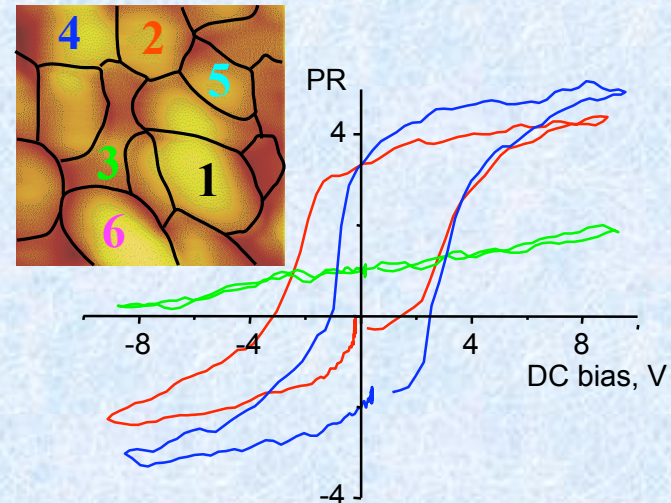
Piezoresponse

Hysteresis Loop: Global Switching vs Local

Polarization Hysteresis Loops



PFM Hysteresis Loops



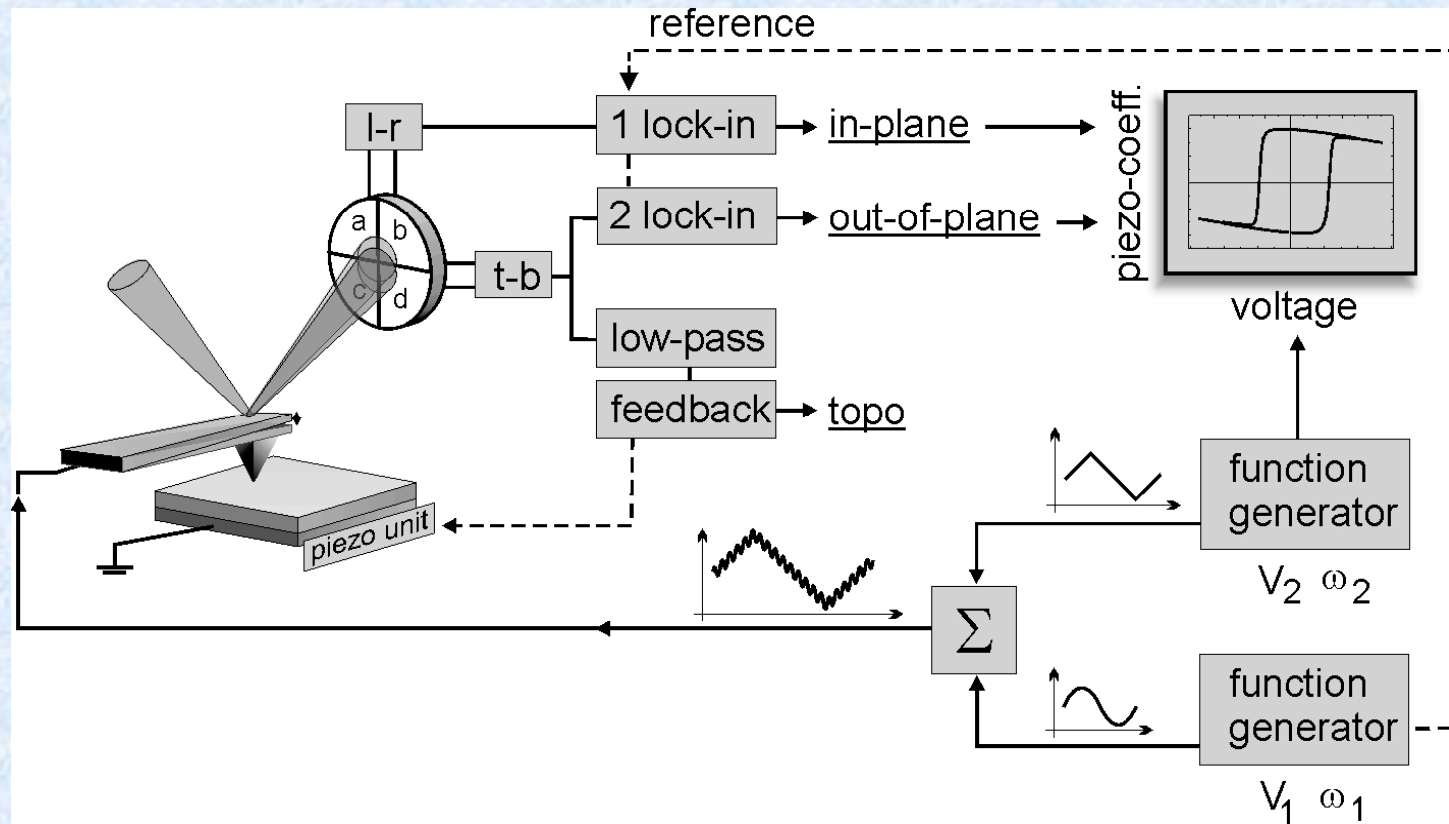
$$PR = d_{\text{eff}} \{V_0 - 2V_w\}$$

Kalinin et al, APL (2004)

Local vs Global Excitation (Thin Films vs Capacitors)

METHOD OF EXCITATION	ADVANTAGES	DRAWBACKS
Local (through the tip)	High lateral resolution Correlation between domain patterns and microstructure Control of nanoscale domains Analysis of domain wall structure and its interaction with microstructural features	Homogeneous electric field Possible effect of surface contamination Difficult to quantify Asymmetric boundary conditions
Integral (through the top electrode)	Homogeneous electric field No electrostatic contribution Quantitative characterization	Lower lateral resolution Detrimental effect of top electrode on imaging resolution

Setup for PFM hysteresis loop measurements

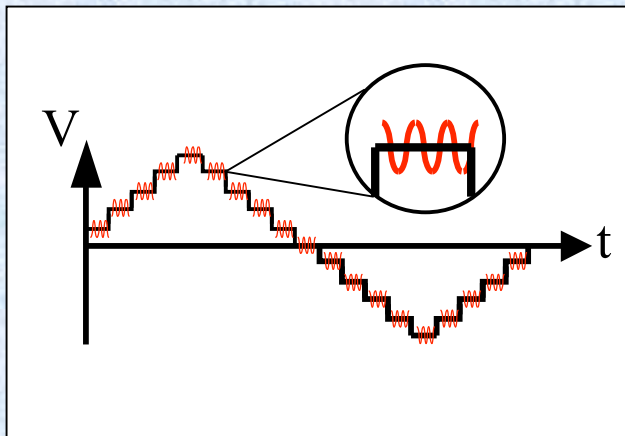


Two function generators and a summation amplifier are used to superimpose the PFM imaging voltage $V_1(\omega_1)$ to the slow (quasi-dc) voltage $V_2(\omega_2)$. The in-plane and out-of-plane signals from the PFM are plotted in an oscilloscope vs the switching voltage V_2 to obtain the piezoelectric hysteresis loops.

Local Hysteresis Loop Measurements in PFM

Two different measurement procedures

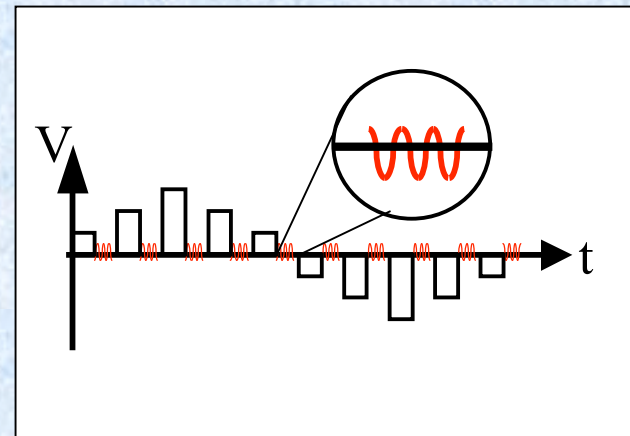
Step mode



In this mode, PFM signal can be affected by capacitance signal, hence it is more suitable for capacitors

Local PFM data can be directly related to the average macroscopic response

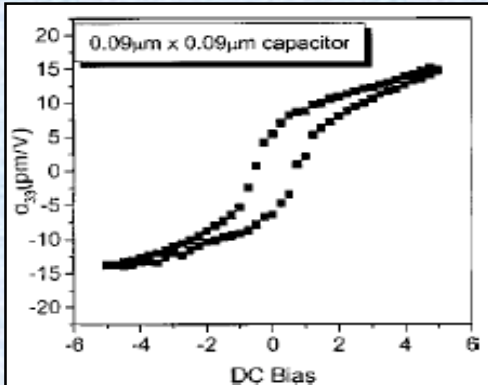
Pulse mode



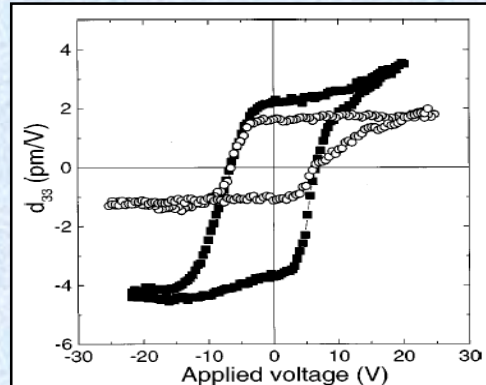
Capacitance signal is less significant, hence, it can be applied to thin films

Measurements can be affected by the backswitching effect

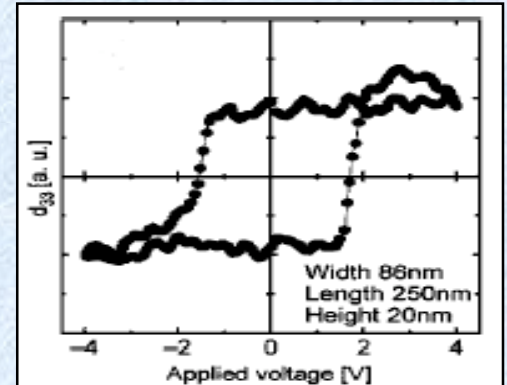
Ferroelectric Nanostructures



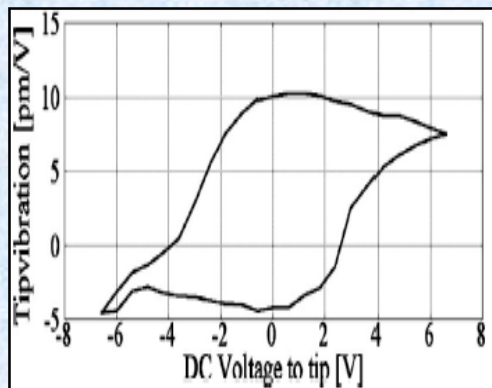
FIB-fabricated PZT capacitor
Ganpule et al, APL 75 (1999)



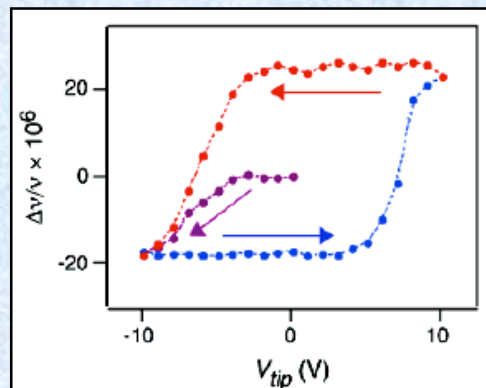
PZT cell array
Alexe et al, APL 75 (1999)



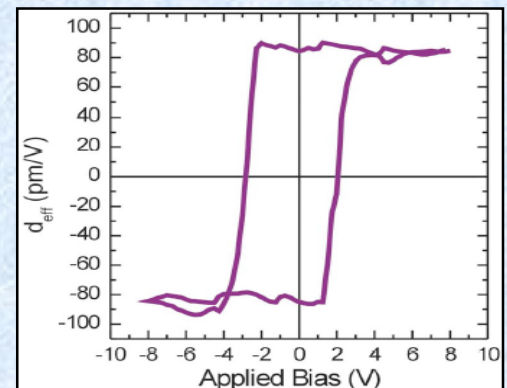
PbTiO₃ nanoislands
Nonomura et al, APL 86 (2005)



PbTiO₃ nanoislands
Buhlmann et al, APL 84 (2004)



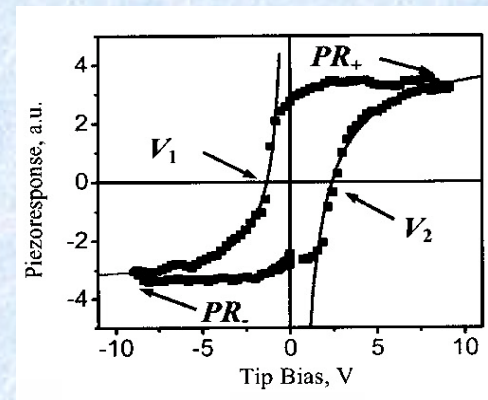
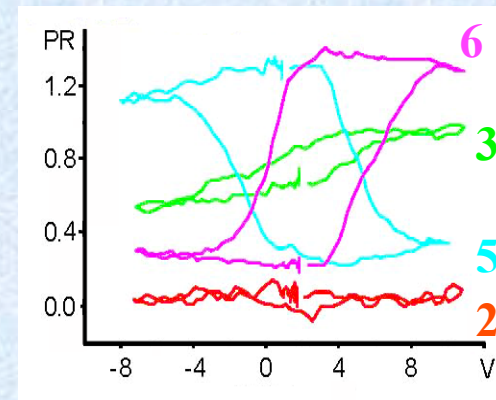
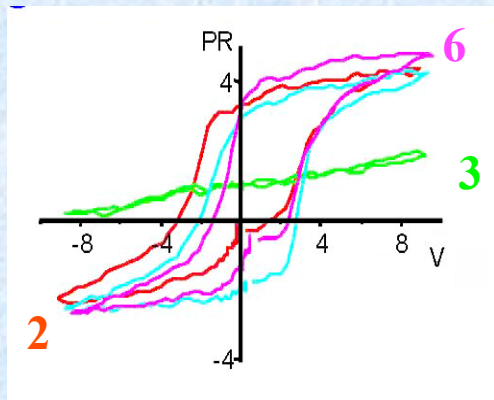
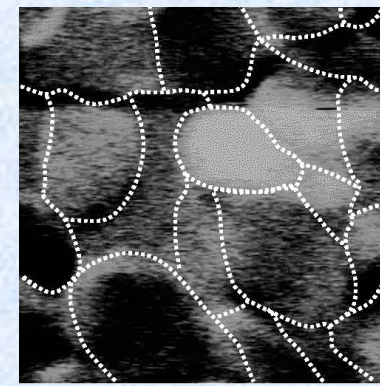
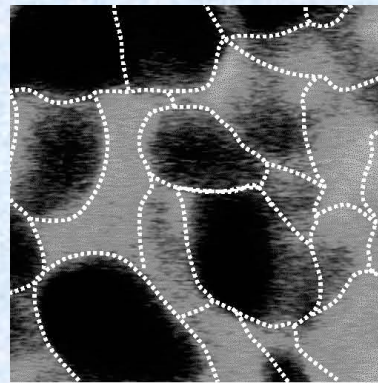
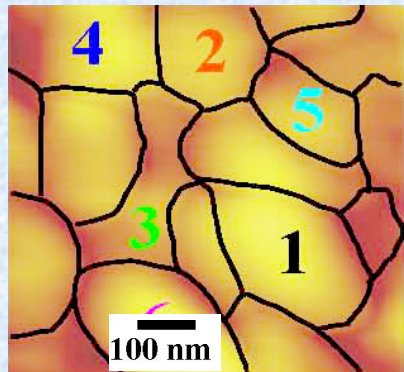
BaTiO₃ nanowire
Yun et al, Nano Letters 2 (2002)



SBT nanotubes
Morrison et al, J. Phys. Cond. Matt. 15 (2003)

PFM allows testing the switching behavior of ferroelectric nanostructures

Local hysteresis Loop: Effect of Grain Orientation



Grain 2: Ferroelectric, Large P_{out} , zero P_{in}

Grain 3: Non-ferroelectric or fully in-plane

Grain 5: Ferroelectric, large P_{out} , left P_{in}

Grain 6: Ferroelectric, large P_{out} , right P_{in}

$$-\tilde{A}_{\text{piezo}} = \alpha \int_0^\infty d_{33} E_z dz = \alpha d_{33} \left\{ \int_0^l E_z dz - \int_l^\infty E_z dz \right\}$$

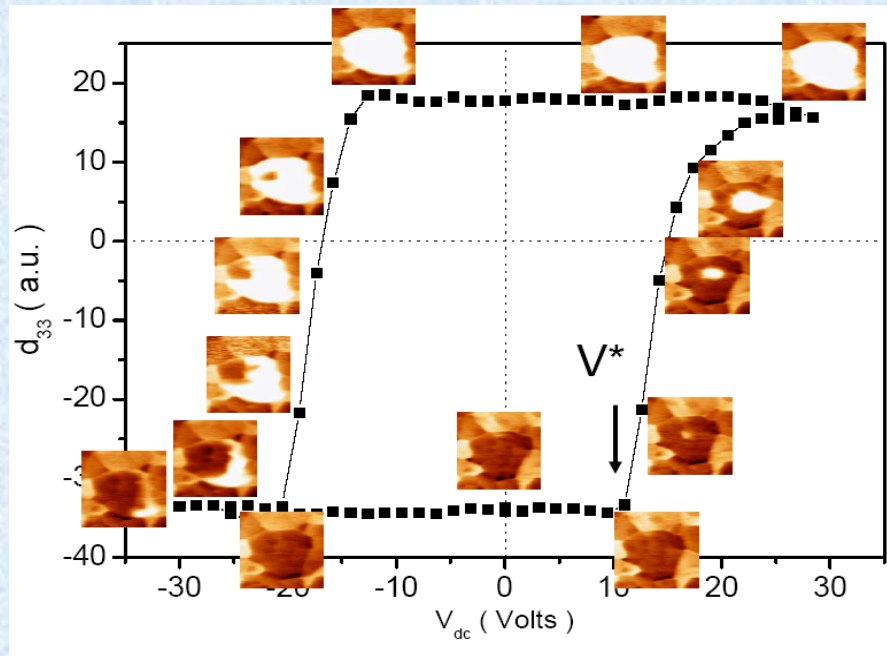
$$PR = \alpha d_{33} (1 - \beta / V_{dc})$$

$$d_{zz} \sim d_{33} \cos^3 \theta$$

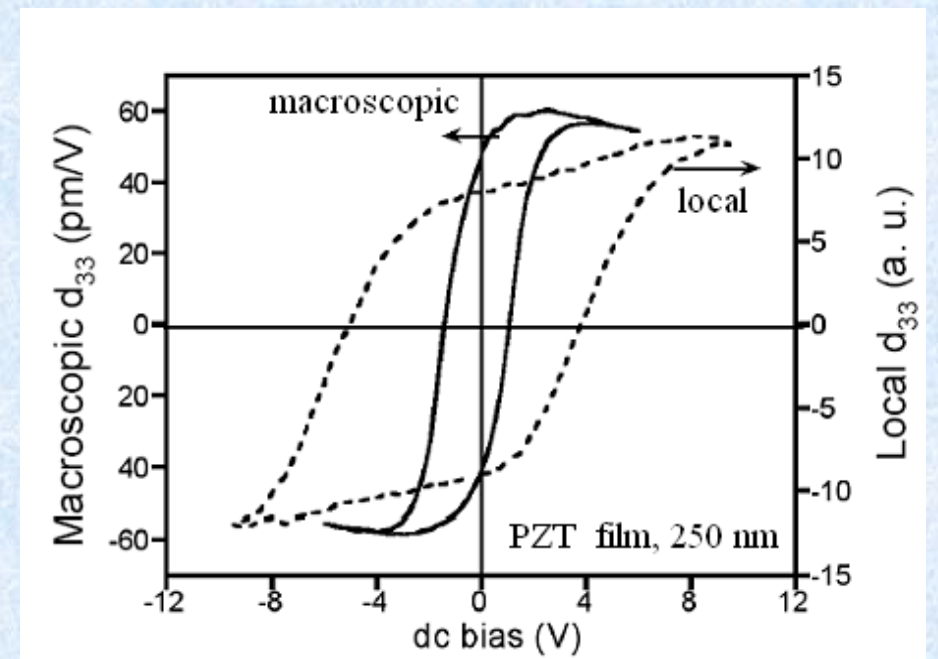
Kalinin, Gruverman, Bonnell, APL (2004)

PFM hysteresis loop: correlation with local domain poling

A local PFM loop of a PZT film and corresponding domain structures

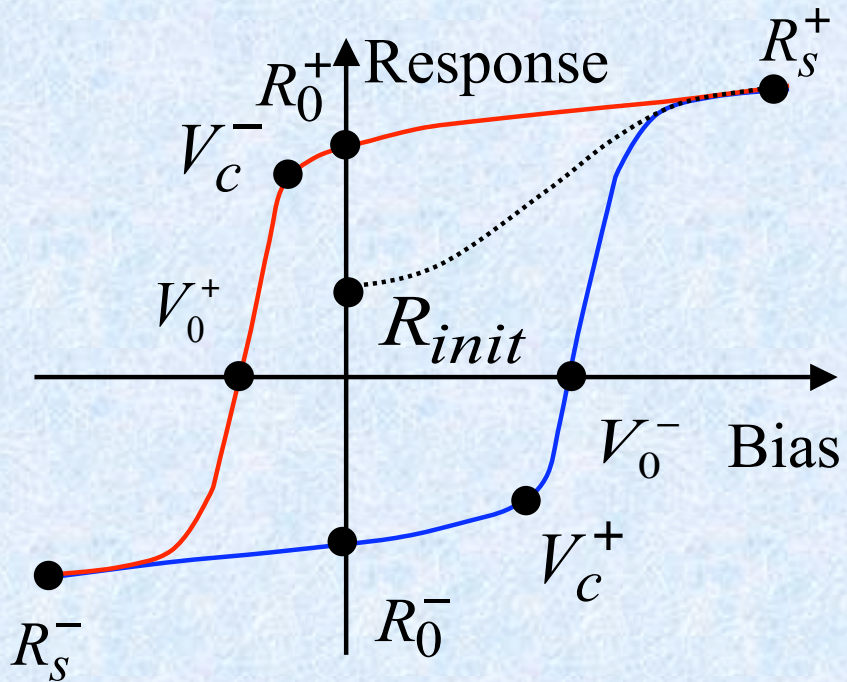


Local PFM and macroscopic loops measured in a PZT thin film



Coercive voltage is different in macroscopic and PFM switching conditions illustrating different physical meanings.

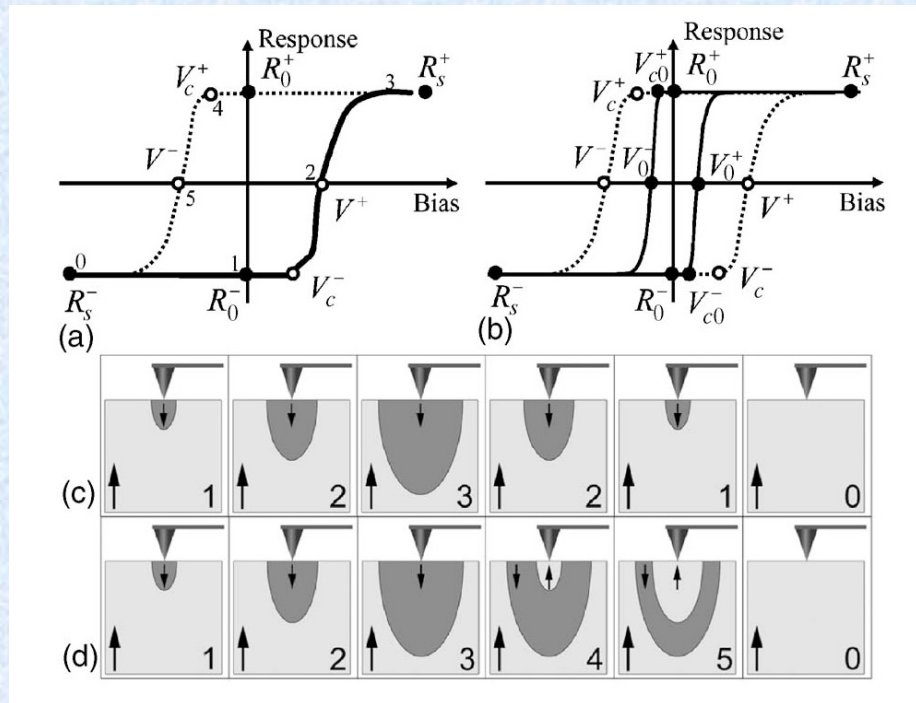
Data Analysis in PFM Switching Spectroscopy



R_{init}	PFM image
V_0^+	Positive coercive bias
V_0^-	Negative coercive bias
V_{c0}^+, V_{c0}^-	Nucleation bias
$\text{Im} = \frac{V_0^+ + V_0^-}{2}$	Imprint
R_0^+, R_0^-	Remanent polarization
R_s^+, R_s^-	Saturated response
$R_m = R_s^+ - R_s^-$	Switchable polarization
$A_s = \int_{-\infty}^{+\infty} (R^+(V) - R^-(V)) dV$	Work of switching

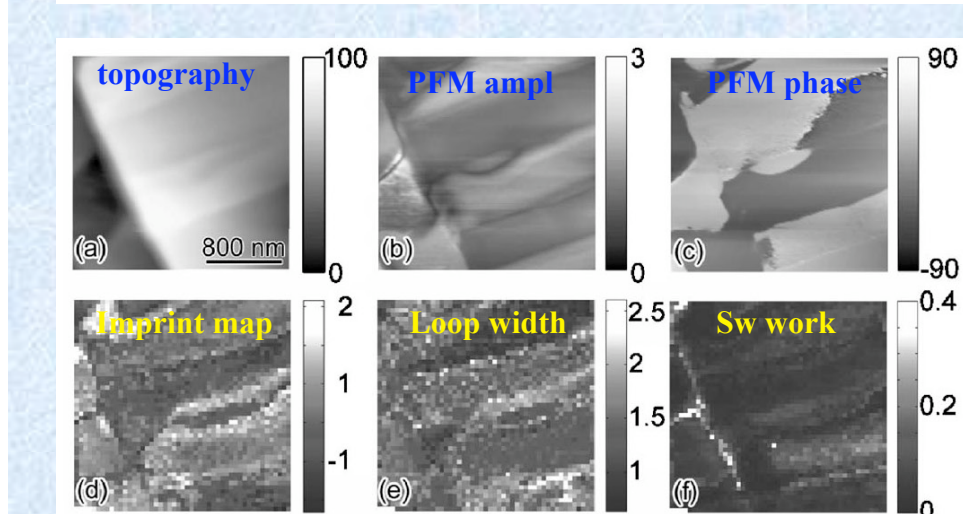
1. Statistical analysis
2. Direct curve fitting

Local PFM Switching Spectroscopy



$$PR = d_{eff} \{1 - k / (P_s V_{dc})\}$$

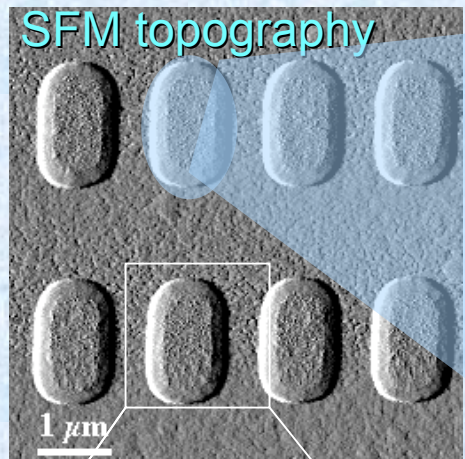
Modeling of local PFM loop allows detection of maximum switchable polarization as well local imprint bias and nucleation threshold.



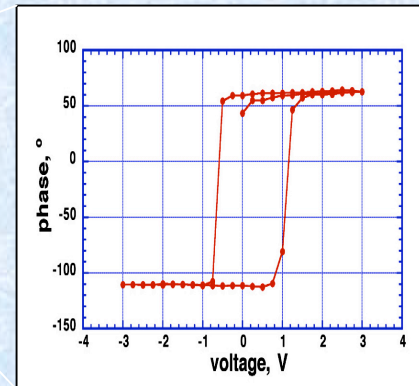
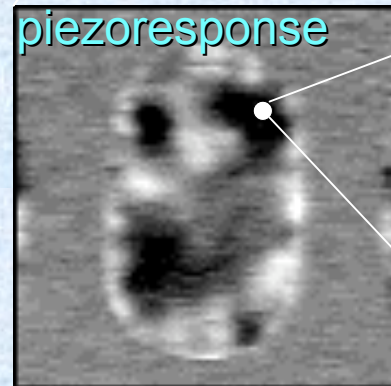
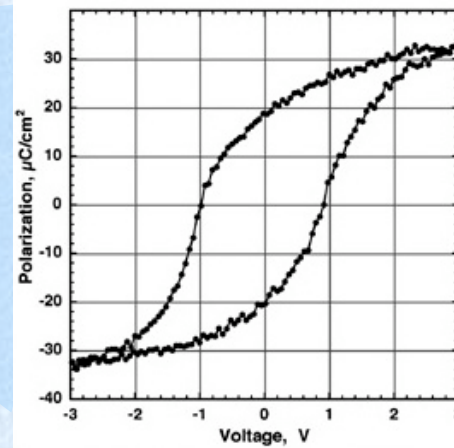
Jesse, Baddorf, Kalinin, APL (2006)

PFM Spectroscopy of FeRAM Capacitors

FeRAM PZT capacitors

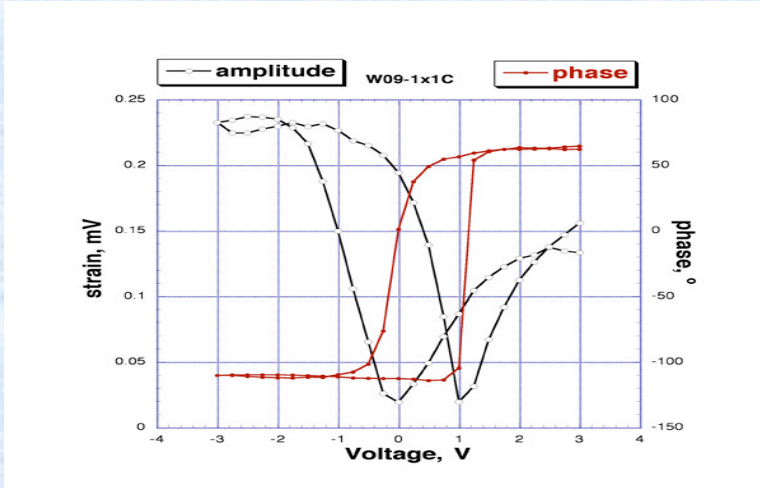


Polarization loop

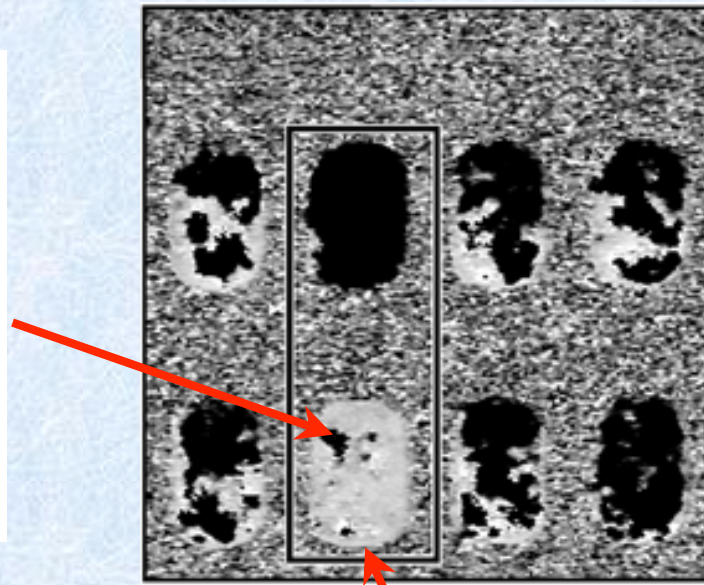


PFM allows a nano-insight into the μm size FeRAM capacitors to address the spatial variability of properties at nanoscale (< 10 nm)

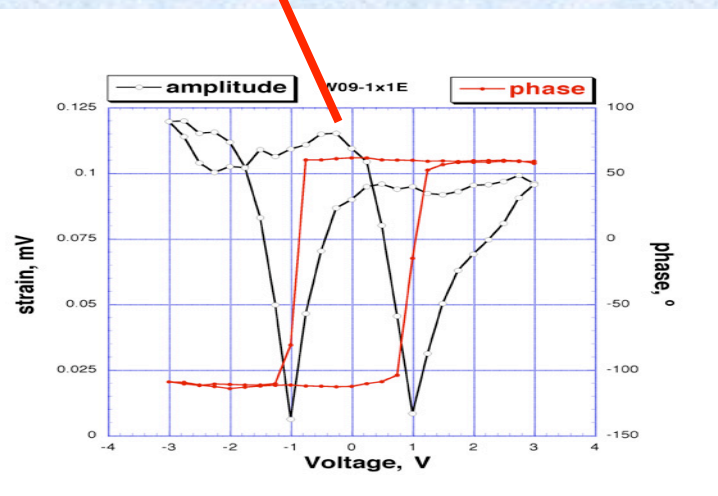
Local PFM Spectroscopy of FeRAM Capacitors



Loops for imprinted region



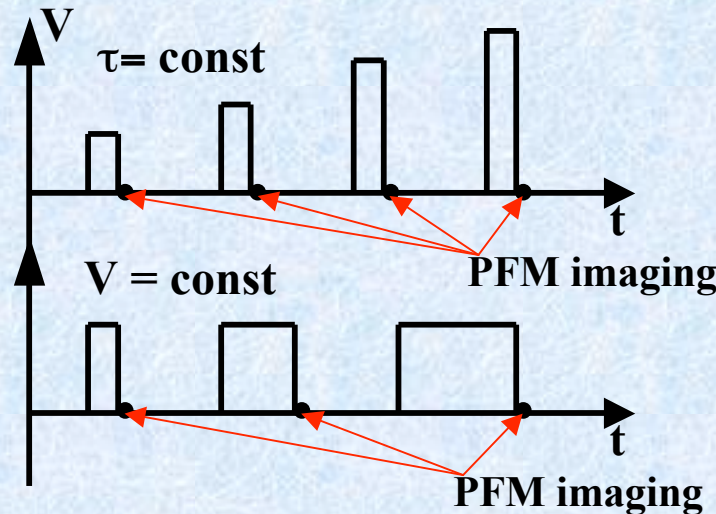
PFM spectroscopy allows a nano-insight into the FeRAM capacitors to address the spatial variability of properties at nanoscale (< 10 nm)



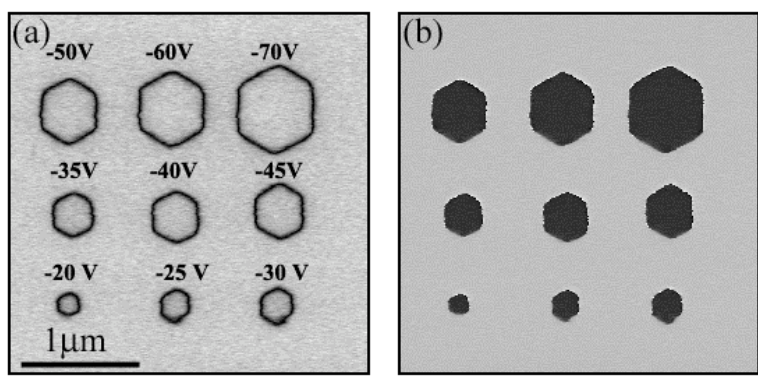
Loops for switchable regions

Local Switching: Domain Growth Kinetics

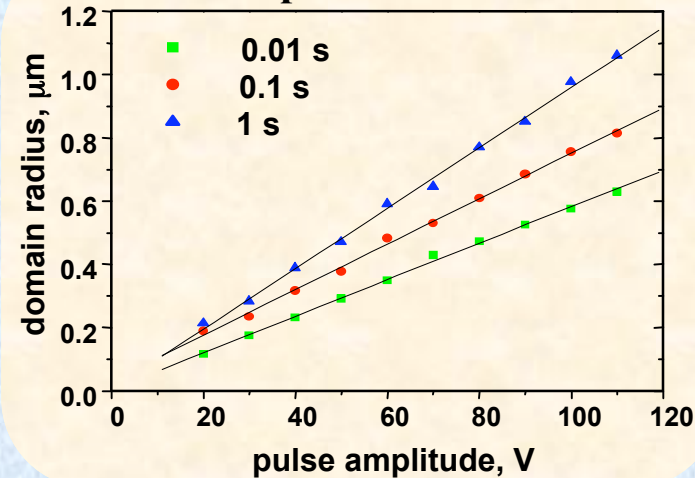
Pulse trains for PFM studies of domain kinetics



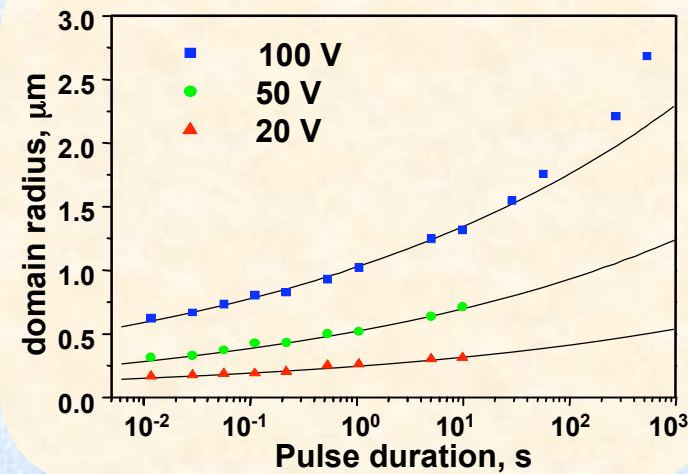
LiNbO_3 ($\tau=10$ ms)



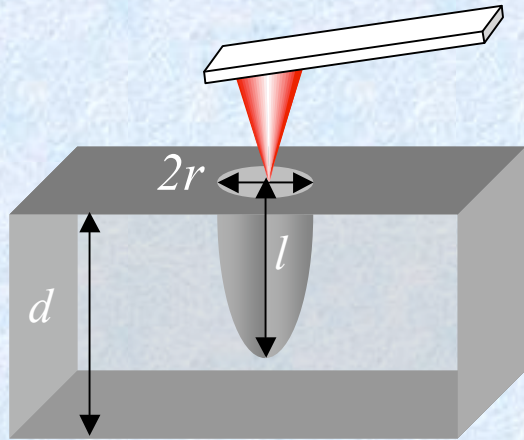
Bias dependence of radius



Time dependence of radius



Domain Growth in Nonuniform Field: Bulk Crystal



$$E(r, \delta) = \frac{C_t V_t}{2\pi\epsilon_0 \sqrt{\epsilon_a \epsilon_c}} \sqrt{\frac{\epsilon_a}{\epsilon_c}} \frac{R_t + \delta}{[(R_t + \delta)^2 + r^2]^{\frac{3}{2}}}$$

Domain energy:

$$\Delta G = -\Delta G_{el} + \Delta G_s + \Delta G_{dep}$$

For bulk crystal ($r \ll l \ll d$)

$$\Delta G_{dep} = \frac{cr^4}{l}; \quad \Delta G_s = brl$$

where

$$c = \frac{16\pi P_s^2}{3\epsilon_a} \left[\ln \left(\frac{2l}{r} \sqrt{\frac{\epsilon_a}{\epsilon_c}} \right) - 1 \right]; \quad b = \frac{\pi^2}{2} \sigma_{wall}$$

For equilibrium domains

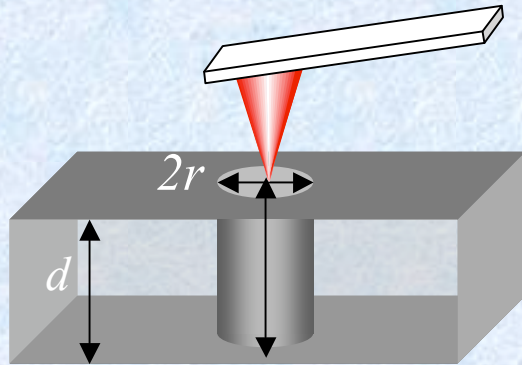
$$r_m = \left(\frac{f^2}{5bc} \right)^{\frac{1}{3}} \quad l_m = \frac{f}{5b}$$

$$f = \frac{8\pi P_s C_t}{\sqrt{\epsilon_a \epsilon_c} + 1} V_t$$

$$r_m \propto V_t^{\frac{1}{3}} \quad l_m \propto V_t$$

Landauer, JAP (1957)
Molotskii, JAP (2003)

Domain Growth in Nonuniform Field: Thin Crystal



For thin crystal ($r > l = d$)

$$\Delta G_{dep} = \alpha r^2 d; \quad \Delta G_s = 2\pi r d \sigma_w$$

where $\alpha = \frac{4\pi^2 P_s^2}{\sqrt{\varepsilon_a \varepsilon_c} + 1}$

For equilibrium domains

$$r_m(V) = \frac{4\pi P_s (V_t - V_{min})}{\alpha d (\sqrt{\varepsilon_a \varepsilon_c} + 1)}$$

V_{min} - threshold voltage to initiate domain formation

This relation holds if the pulse duration is long enough for the domain to reach equilibrium dimension.

For 0.9 μm thick LNO at $V_t=20$ V, $r_m=4$ μm

Domain Growth Kinetics

Assume charged sphere model for large domains
($r > R_t$)

$$E(r, \delta) = \frac{C_t V_t}{2\pi\epsilon_0 \sqrt{\epsilon_a \epsilon_c}} \sqrt{\frac{\epsilon_a}{\epsilon_c}} \frac{R_t + \delta}{[(R_t + \delta)^2 + r^2]^{3/2}}$$

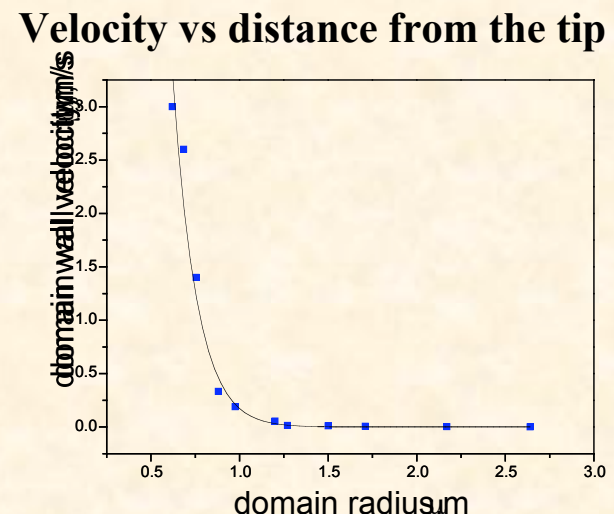
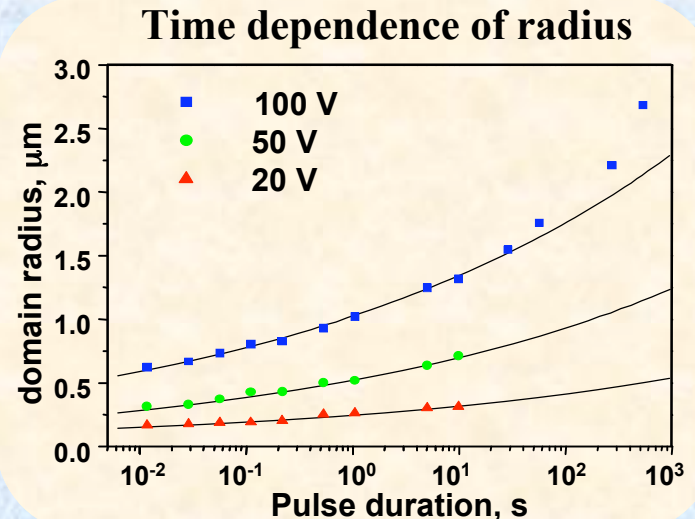
Assuming activation type of wall motion

$$\frac{dr}{dt} = v_\infty \exp(-\delta / E(r))$$

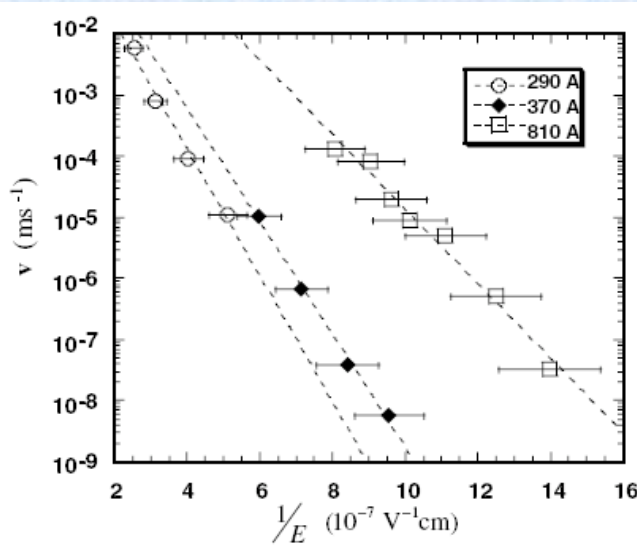
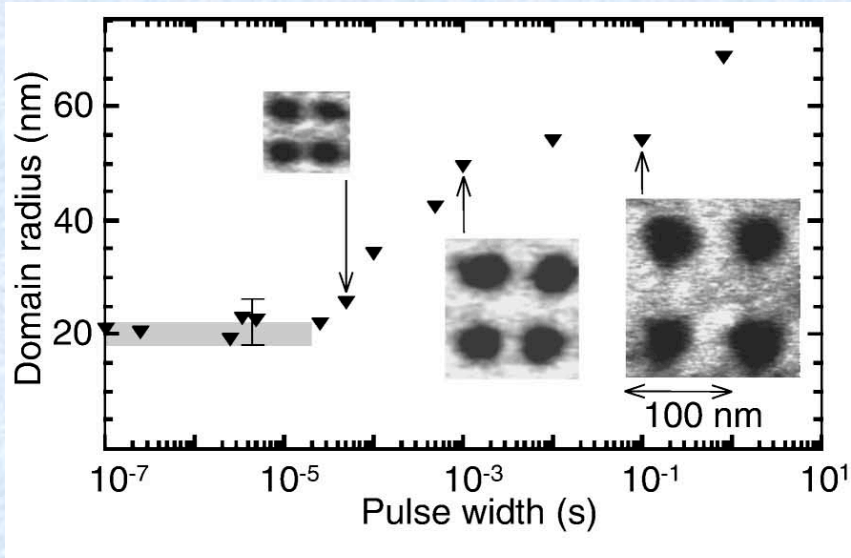
For $r \ll r_m$ time dependence of domain size can be found as

$$r(t) = \frac{r_m}{\eta} \ln \left(1 + \frac{2v_\infty t}{\eta r_m} \right)$$

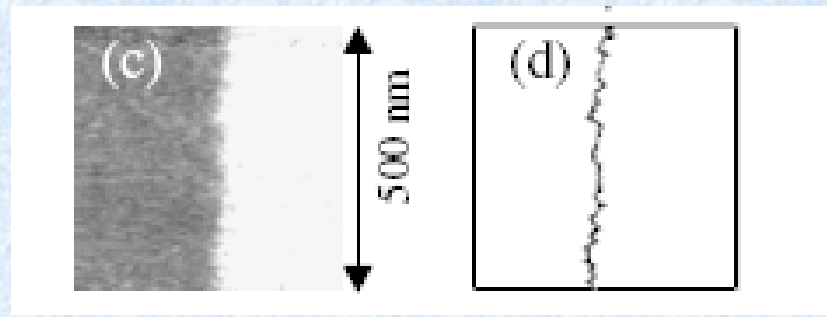
where $\eta = \frac{2\pi P_s \alpha}{\sqrt{\epsilon_a \epsilon_c} + 1}$



Domain Growth Kinetics in Thin Films



$$v \sim \exp - \frac{R}{k_B T} \left(\frac{E_0}{E} \right)^\mu,$$



- Domain growth kinetics can be described as domain wall motion in disordered media
- Kinetics yields information on disorder type
- Similar information can be obtained from wall roughness

Paruch, et al, PRL (2005)
Tybell et al, PRL (2002)

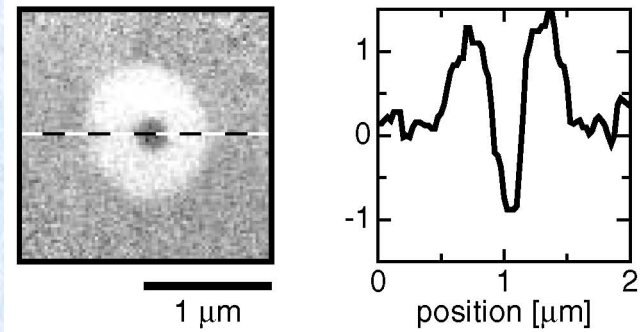
Abnormal Domain Switching in PFM

“Abnormal” switching in PFM - apparent “antipoling” effect when polarization, detected after application of the switching field, is oriented opposite to the applied field direction

Can be ascribed to:

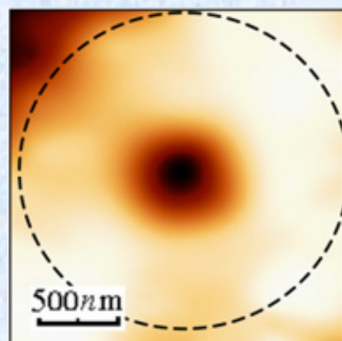
- Effect of the PFM switching conditions
- Inherent switching behavior of the material

BaTiO₃ thin film



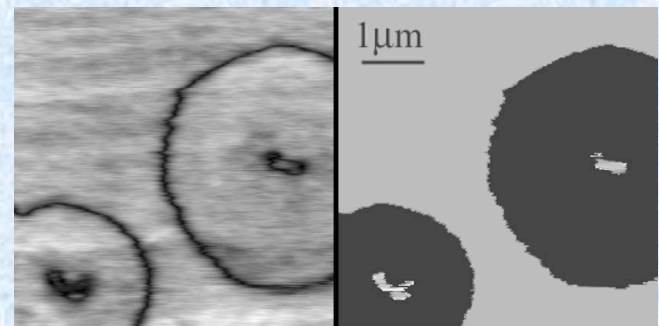
Abplanalp et al, PRL (2001)

PNZT crystal



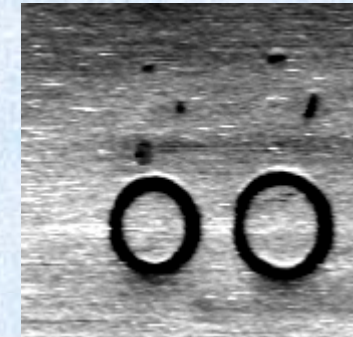
Kholkin et al, Nanotechnology (2007)

Pb(Zr,Ti)O₃ thin film



Buhlmann et al, PR B (2005)

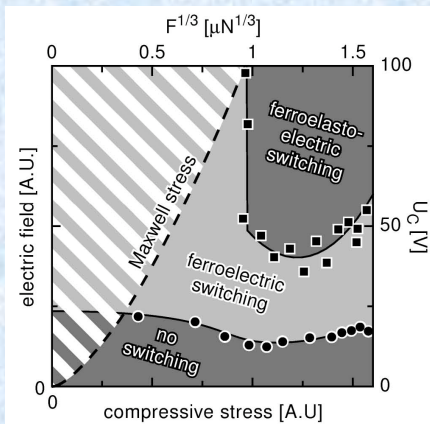
LiNbO₃ crystal



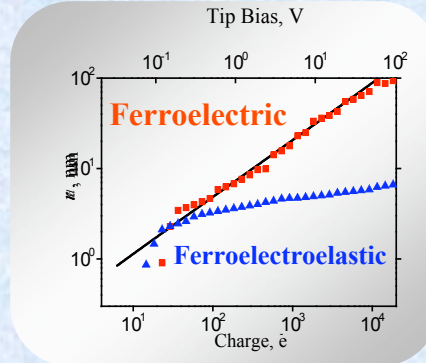
Gruverman et al, Nanotechnology (2008)

Abnormal switching: PFM related-effect

High-order ferroic switching

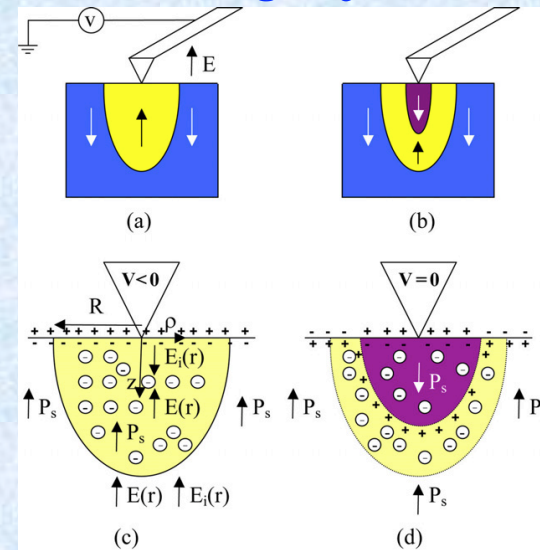


Abplanalp et al, PRL (2001)

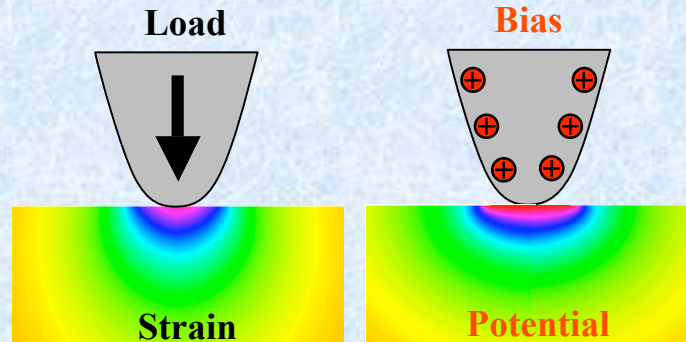


Kalinin et al, JAP (2006)

Charge injection

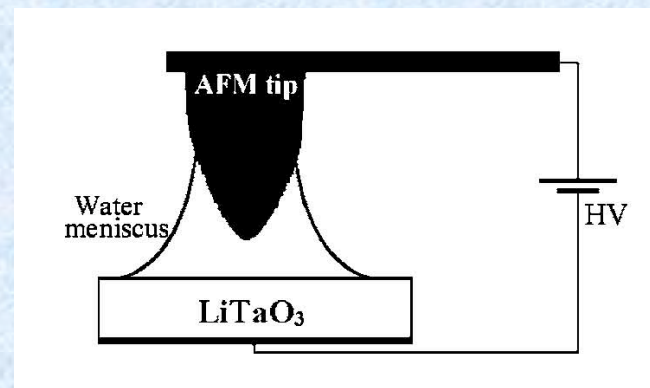


Khoklin et al, Nanotechnology (2007)



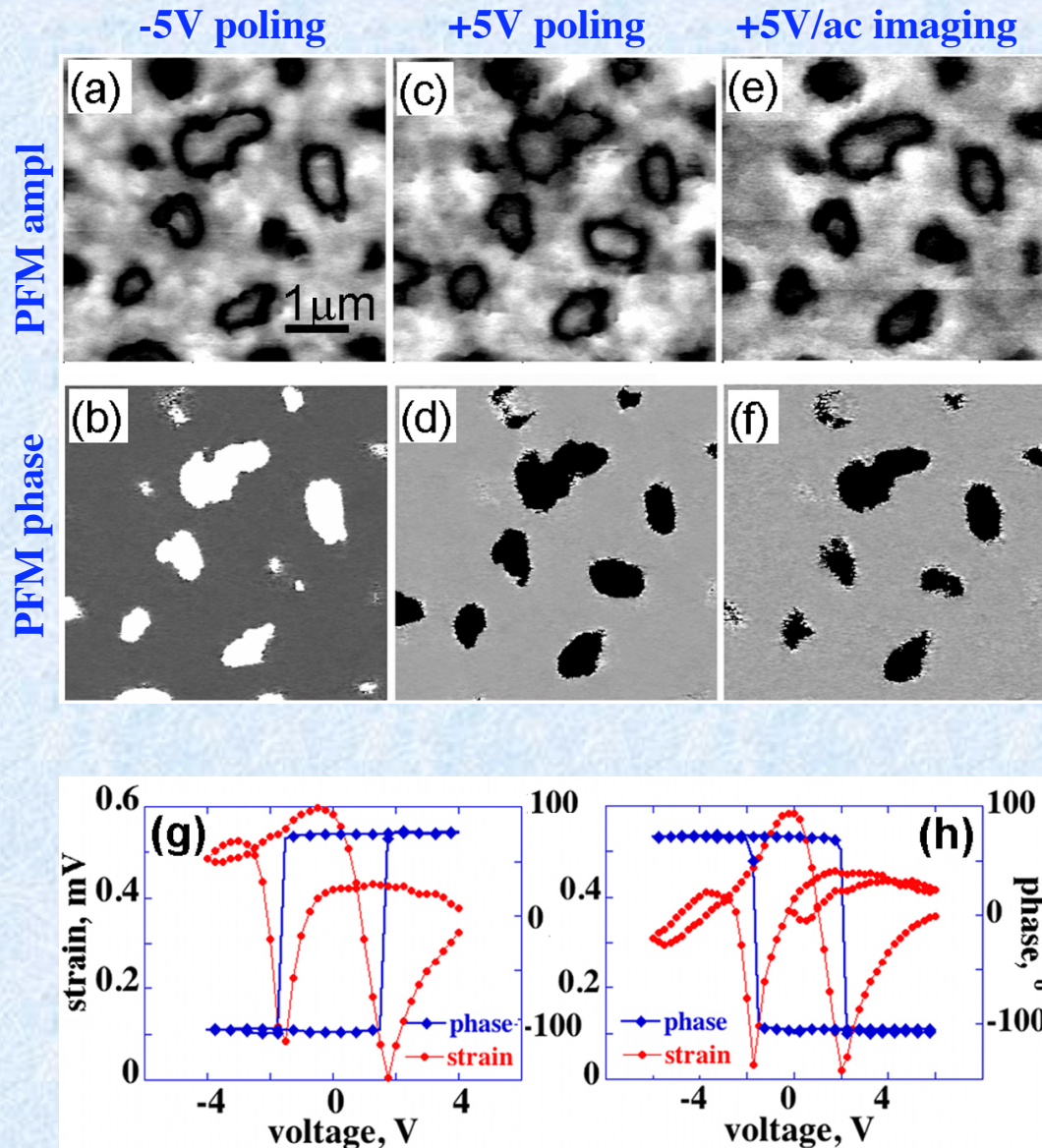
In piezoelectric materials, electrical and mechanical phenomena are coupled

Environment effect



Dahan et al, APL (2006)

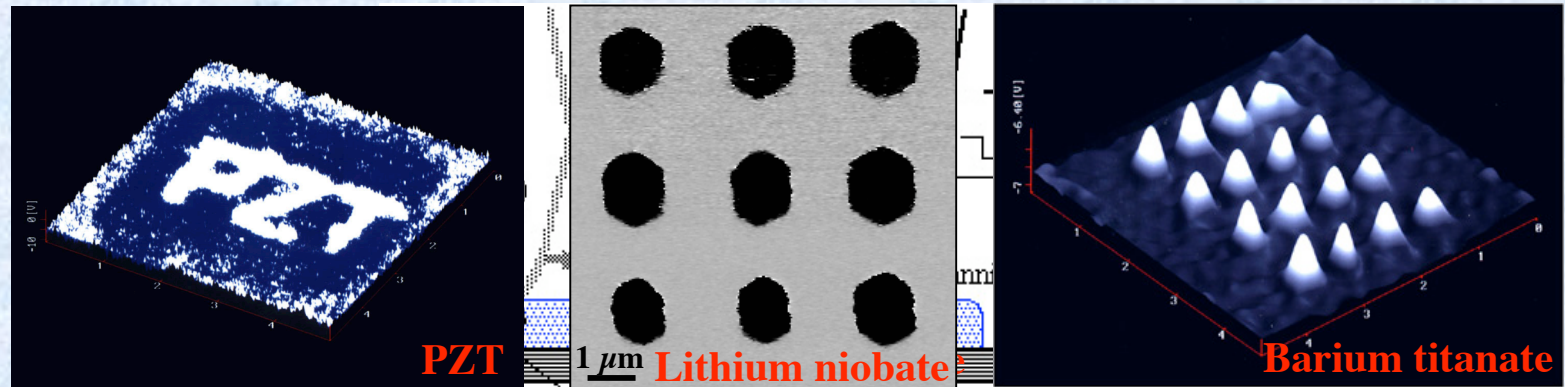
Abnormal Switching: Intrinsic Material Effect



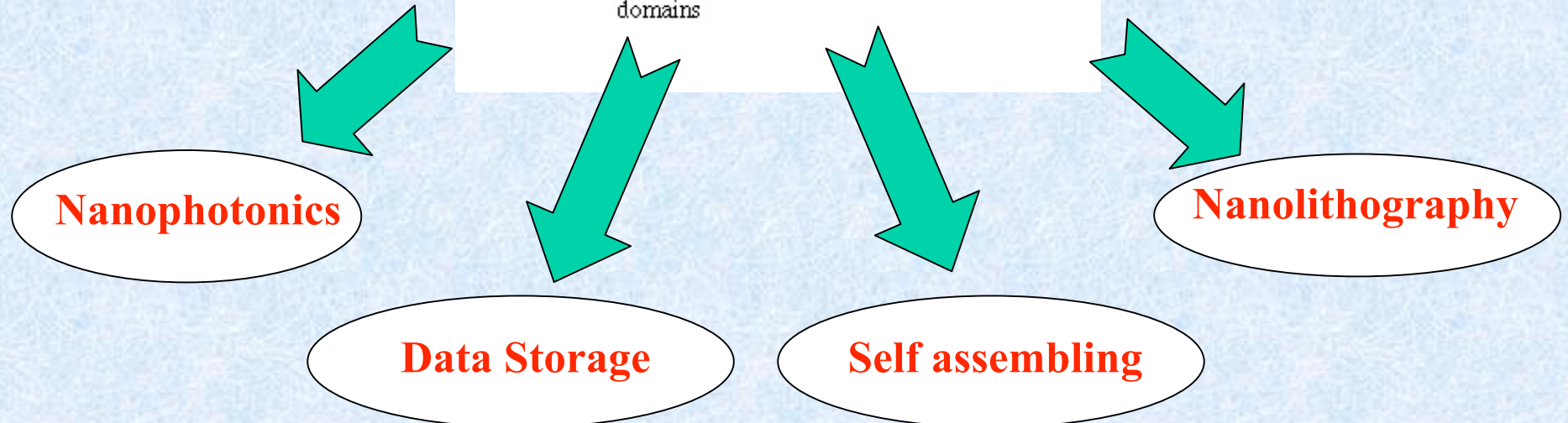
True abnormal switching was observed on PZT capacitors with MPB composition;

It is suggested that the observed effect is due to the combination of charge compensation and mechanical stress effects in the grains with rhombohedral structure.

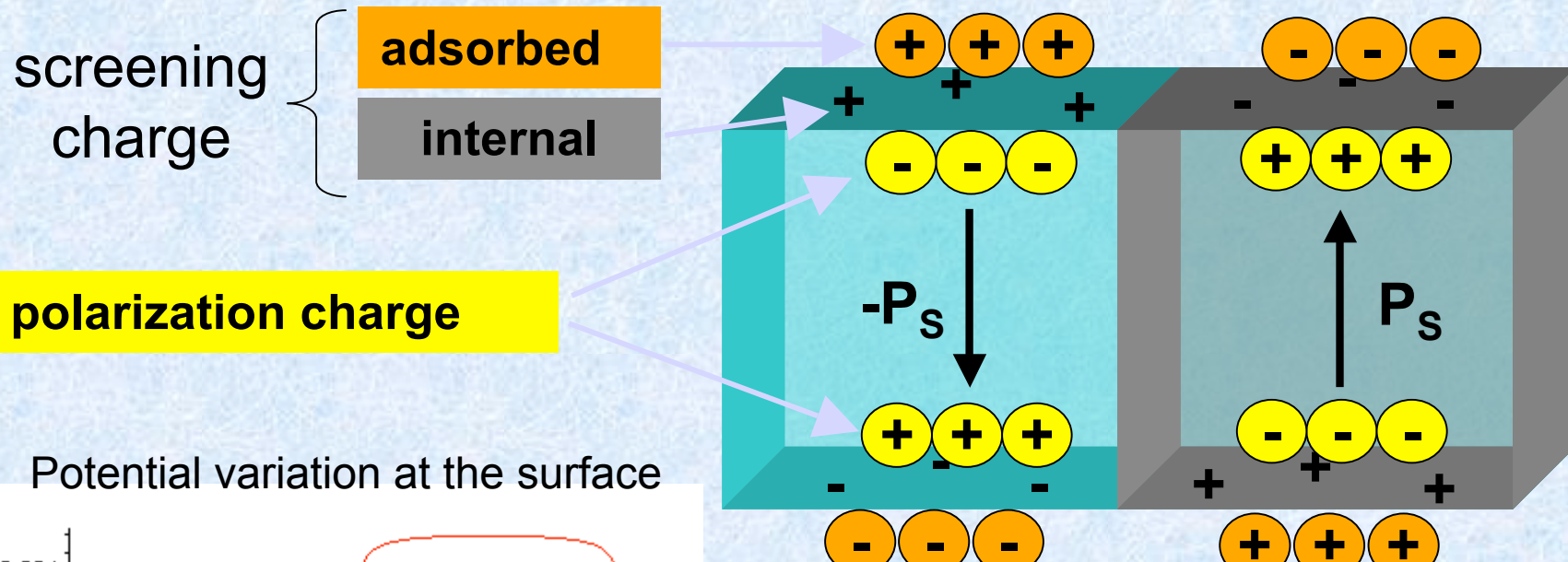
Ferroelectric Templates for Fabrication of Nanostructures



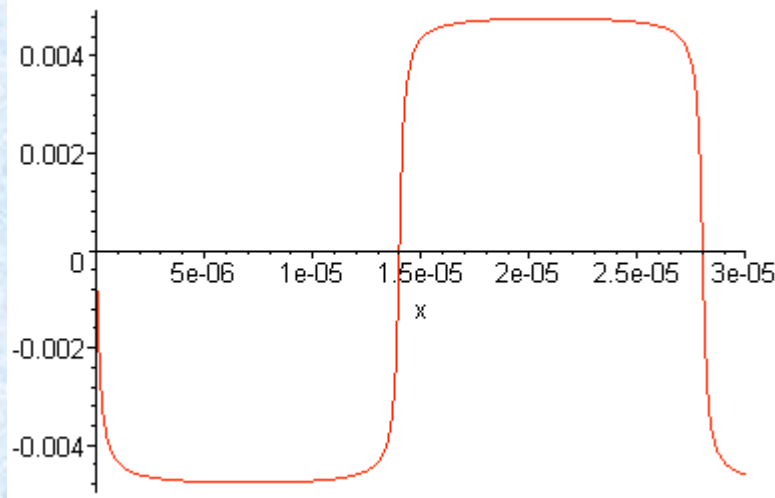
Ferroelectric Domain Patterning by PFM



Polarization Screening on Ferroelectric Surfaces



Potential variation at the surface



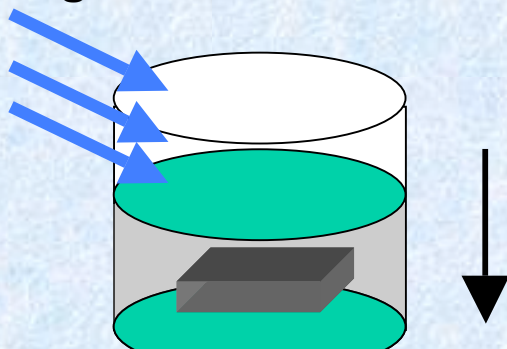
Selective deposition will be driven by a combination of surface charge, surface potential and surface dipoles.

Photoinduced Deposition in Aqueous Solution

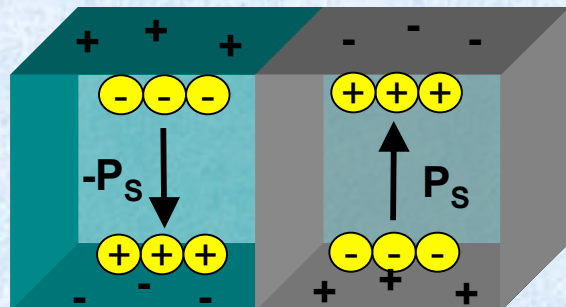
Photochemical reaction

material in ionic solution is illuminated with super band gap light

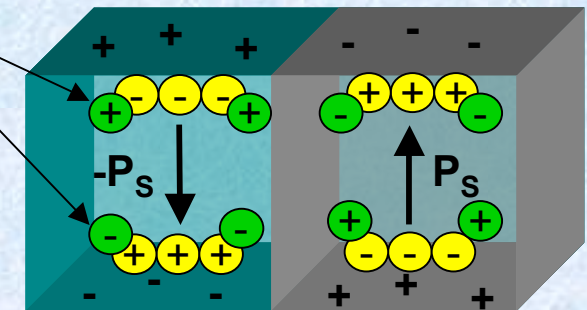
UV light



electron-hole pairs form



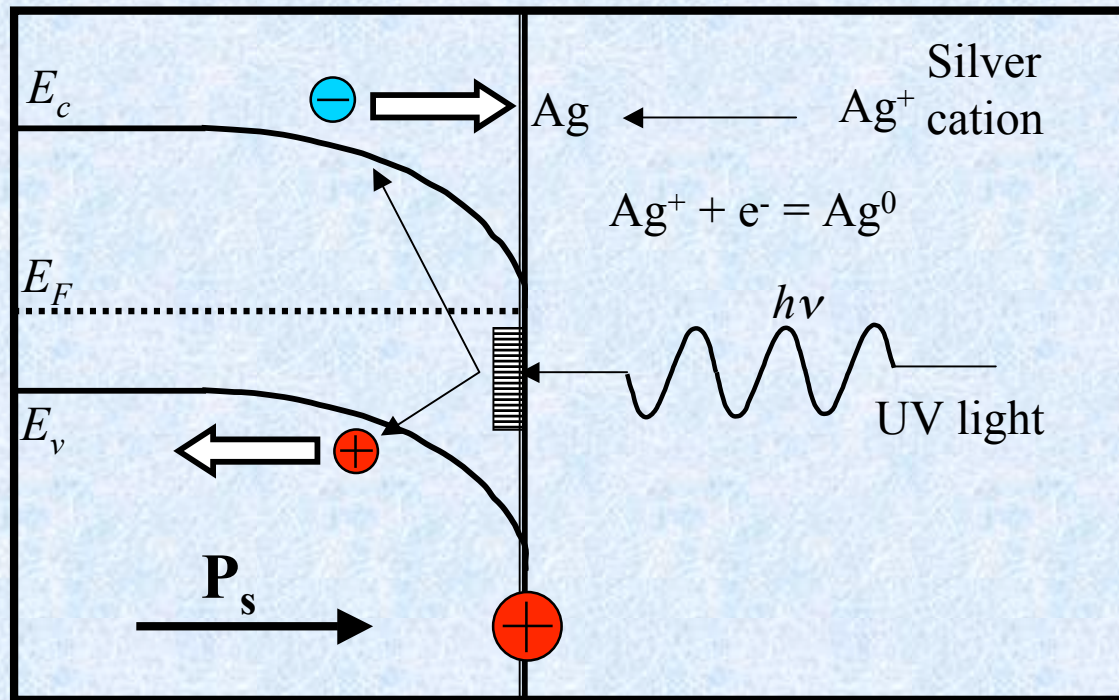
UV generated
charge carriers



deposition is facilitated by surface reduction of metal ions by free charge carriers

Mechanism of Photoinduced Deposition on Ferroelectric

Deposition on PZT film

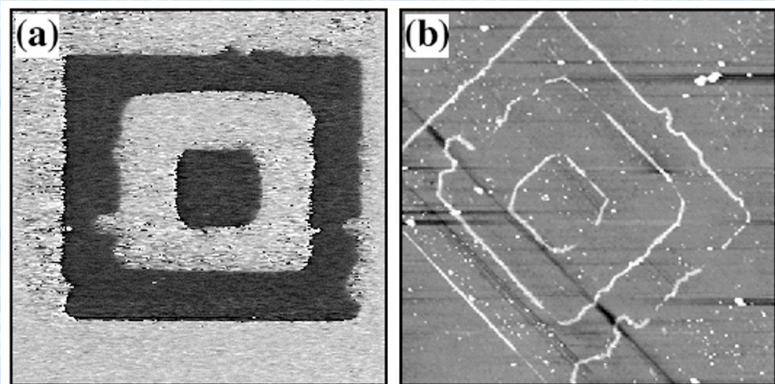


Charge $\sigma_{pol} = \mathbf{P} \cdot \mathbf{n}$

$0.26 \text{ C/m}^2 \sim 0.26 \text{ } e^-/\text{u.c.}$

- Ag reduction occurs on c^+ domains
- Oxidation occurs on c^- domains

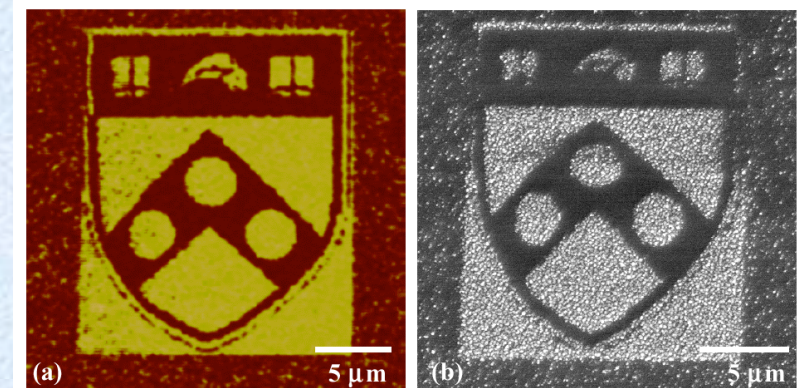
Polarization-controlled Selective Deposition



(a) PFM-generated image in lithium niobate crystal

(b) AFM topography after Ag deposition

J. Hanson et al, APL (2006)



(a) PFM-generated image in PZT thin film (Penn logo).

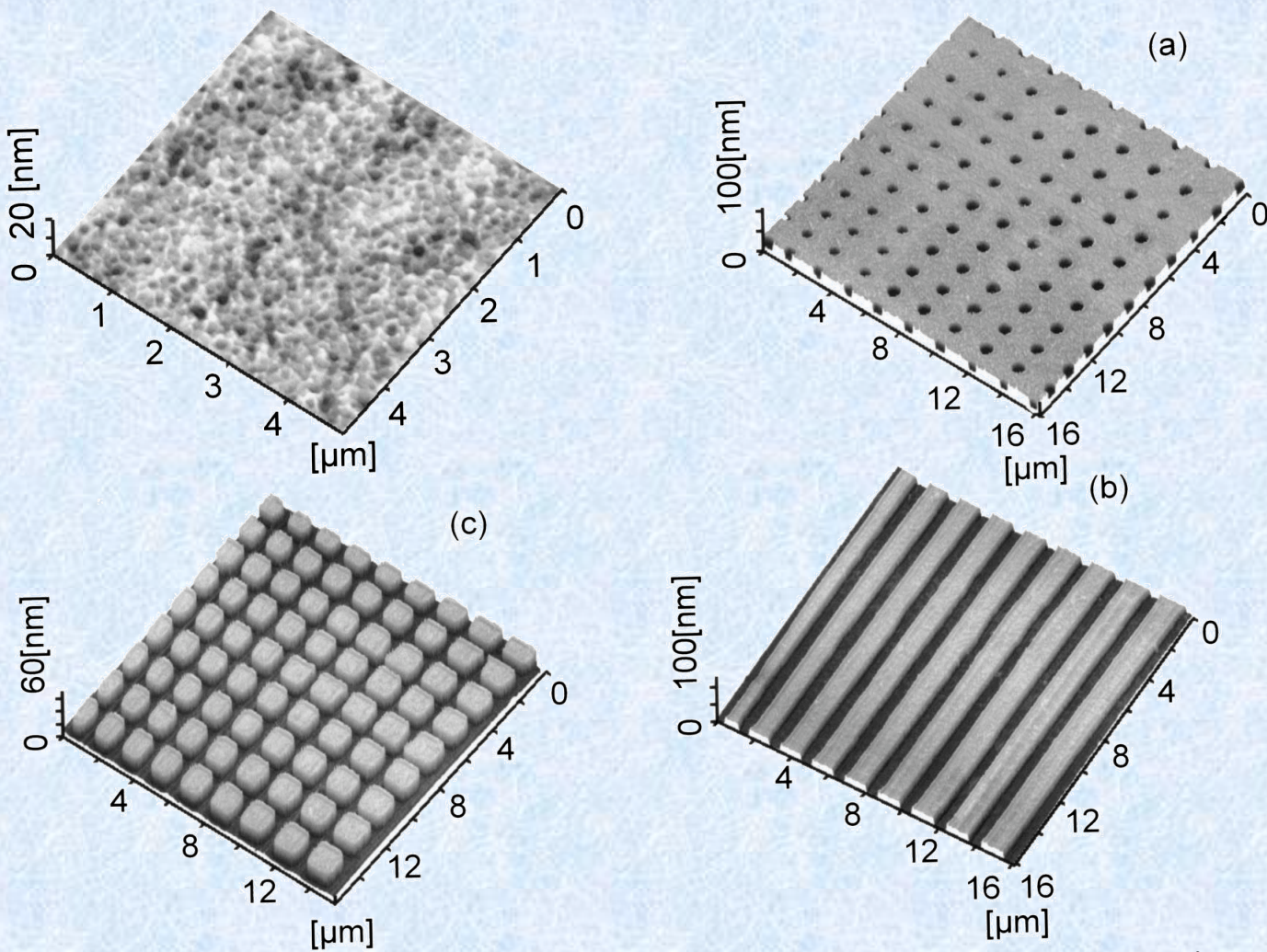
(b) SEM image after silver deposition in c+ domains.

S. V. Kalinin et al, Nano Letters 2 (2002)

High throughput substrate characterization and high-resolution domain patterning are key components of ferroelectric lithography

From Domain Patterns to Nanostructures

- Etching rate of ferroelectric material is dependent on domain orientation
- Etching produces relatively flat (2 nm roughness for 70 nm depth) surfaces



Liu et al, JAP (2005)

Conclusion

PFM spectroscopy allows measurement of local switching parameters and assessment of spatial variation of properties in ferroelectric structures and devices at the nanoscale level.

PFM-based control of ferroelectric domains opens a new route for fabrication of materials with properties tailored at the nanoscale